

1
2
3
4
5
6
7
8
9
10
11
12
13
14
15
16
17
18
19
20
21
22
23
24
25
26
27
28
29

DR. ANNA T. TRUGMAN (Orcid ID : 0000-0002-7903-9711)

DR. WILLIAM R. L. ANDEREGG (Orcid ID : 0000-0001-6551-3331)

Article type : Research Review

Leveraging plant hydraulics to yield predictive and dynamic plant leaf allocation in vegetation models with climate change

Running head: Towards predictive leaf allocation in models

AT Trugman^{1,2,*}, LDL Anderegg^{3,4}, JS Sperry¹, Y Wang¹, M Venturas¹, WRL Anderegg¹

¹*School of Biological Sciences, University of Utah, Salt Lake City, UT 84112, USA;* ²*Department of Geography, University of California Santa Barbara, Santa Barbara, CA 93106, USA;*

³*Department of Global Ecology, Carnegie Institution for Science, 260 Panama St, Stanford, CA 94305, USA;* ⁴*Department of Integrative Biology, University of California Berkeley, Berkeley, CA 94720, USA*

Correspondence:

*A.T. Trugman, tel. 505-500-6604, e-mail: att@ucsb.edu

Key words: Ecohydrological equilibrium, Leaf area, Allocation, Optimization, Plant hydraulics, Vegetation models, Vegetation water demand

Type of Paper: Research Review

This is the author manuscript accepted for publication and has undergone full peer review but has not been through the copyediting, typesetting, pagination and proofreading process, which may lead to differences between this version and the [Version of Record](#). Please cite this article as [doi: 10.1111/GCB.14814](https://doi.org/10.1111/GCB.14814)

This article is protected by copyright. All rights reserved

30

31 **Abstract**

32 Plant functional traits provide a link in process-based vegetation models between plant-
33 level physiology and ecosystem-level responses. Recent advances in physiological understanding
34 and computational efficiency have allowed for the incorporation of plant hydraulic processes in
35 large-scale vegetation models. However, a more mechanistic representation of water limitation
36 that determines ecosystem responses to plant water stress necessitates a re-evaluation of trait-
37 based constraints for plant carbon allocation, particularly allocation to leaf area. In this review,
38 we examine model representations of plant allocation to leaves, which is often empirically set by
39 plant functional type-specific allometric relationships. We analyze the evolution of the
40 representation of leaf allocation in models of different scales and complexities. We show the
41 impacts of leaf allocation strategy on plant carbon uptake in the context of recent advancements
42 in modeling hydraulic processes. Finally, we posit that deriving allometry from first principles
43 using mechanistic hydraulic processes is possible and should become standard practice, rather
44 than using prescribed allometries. The representation of allocation as an emergent property of
45 scarce resource constraints is likely to be critical to representing how global change processes
46 impact future ecosystem dynamics and carbon fluxes and may reduce the number of poorly
47 constrained parameters in vegetation models.

48 **Introduction**

49 Forested regions around the globe represent ~363 Pg C (equivalent to ~170 ppm CO₂ if
50 released to the atmosphere) and sequester ~2.3 Pg C annually, or approximately 25% of annual
51 anthropogenic carbon emissions (Bonan, 2008; Pan et al., 2011). Tree carbon allocation to leaf
52 biomass, and the resultant ratio of leaf area (A_L) relative to sapwood area (area of tree water
53 transport tissue, A_S) influences ecosystem carbon drawdown and water loss through the stomata.
54 Leaf allocation is shaped both by intrinsic plant physiological traits (Bartlett, Scoffoni, & Sack,
55 2012; Choat et al., 2012) and the local environment (Martinez-Vilalta et al., 2009; Mencuccini &
56 Bonosi, 2001; Mencuccini & Grace, 1994). However, due to the elusive nature of the biological
57 mechanisms underlying tree leaf allocation, vegetation models often determine A_L using fixed
58 coefficients or scaling laws. Uncertainty in leaf allocation strategy introduced using fixed
59 coefficient or scaling law methods impacts A_L projections, the ratio of $A_L:A_S$, and the sensitivity
60 of vegetation productivity to environmental drivers.

61 The objective of this review is to provide an overview of how leaf allocation strategy is
62 represented in current state-of-the-art numerical vegetation models, how allocation impacts
63 internal plant water stress, and ultimately how allocation is tied to predictions for terrestrial
64 productivity. First, we discuss the theory, history and fundamental limitations of the use of
65 allometric equations, which are a common technique used to standardize leaf biomass allocation
66 estimates among species or plant functional groups. Second, we examine the different
67 representations of plant carbon allocation to leaves in vegetation models ranging in scales and
68 complexities from single plant models to ecosystem models and large-scale vegetation models.
69 Third, we provide context on the role of leaf allocation in the physiology of plant water
70 limitation. Fourth, we propose a way for moving forward with prognostic leaf allocation in large-
71 scale models to improve predictive abilities for plant productivity and water stress. We conclude
72 with a discussion on how the plant hydraulics framework presented here can inform the global
73 optimization problem of understanding allocation broadly in the presence of multiple limiting
74 resources.

75

76 **Allometric biomass equations: history & theory**

77 The fields of forestry and ecology rely heavily on allometric regression equations, which
78 relate tree size to plant biomass to quantify species-specific allocation strategies. Numerous
79 species- and site-specific allometric regression models have been developed over the years,
80 beginning in prevalence the 1960s, that document the relationships between tree size (often
81 diameter at breast height, dbh, or diameter at tree base) and plant biomass components including
82 total aboveground tree biomass, stem biomass, bark biomass, branch biomass, and leaf biomass
83 (Baskerville, 1972; Chave et al., 2014; Jenkins, Chojnacky, Heath, & Birdsey, 2003; Ploton et
84 al., 2016; Ter-Mikaelian & Korzukhin, 1997; Whittaker & Woodwell, 1968; Zianis, Muukkonen,
85 Mäkipää, & Mencuccini, 2005). These equations are useful for many applications, however
86 literature-reported single-species allometric regression model performance is often no better at
87 predicting out-of-sample tree allometries than multi-species models because of the wide
88 intraspecific variations in allocation due to local environmental conditions (Fayolle, Doucet,
89 Gillet, Bourland, & Lejeune, 2013; Lines, Zavala, Purves, & Coomes, 2012). Indeed, it has been
90 documented that the largest source of error in scaling from trees to forests biomass estimates is
91 error associated with allometric model choice, rather than errors in tree measurement or sampling

92 uncertainty associated with plot size or composition (Chave et al., 2004). Further, general
93 allometry equations perform particularly poorly when predicting local leaf or tree crown biomass
94 (Bond-Lamberty, Wang, & Gower, 2002; Ploton et al., 2016), making allometric regression
95 models inaccurate when determining tree allocation strategies to leaves, and consequently
96 increasing tree $A_L:A_S$ uncertainty in out-of-sample environmental conditions. Indeed, the need to
97 use ‘local’ allometric equations or to validate equations locally has long been emphasized in the
98 forestry literature (Ketterings, Coe, Van Noordwijk, Ambagau, & Palm, 2001).

99 Thus, a fundamental question arises: how much does leaf allocation (and $A_L:A_S$) vary
100 within a species for trees of equivalent size? A recently published Biomass And Allometry
101 Database (BAAD) for woody plants (Falster et al., 2015) provides initial insights and has strong
102 potential for improving our understanding of the complexity of the underlying biotic and abiotic
103 factors driving plant allocation. The BAAD is a compilation of individual-level allocation data
104 from numerous previously-published studies that span thousands of individual woody plants,
105 hundreds of species, and different growth environments around the globe. Though the number of
106 observations with concurrent documentation of A_L and A_S for a given tree within the BAAD are
107 relatively sparse (863 observations), assuming tree trunk basal area (BA) as proportional to A_S
108 (i.e. $\frac{A_L}{BA} \propto \frac{A_L}{A_S}$, where $BA = \pi\left(\frac{dbh}{2}\right)^2$) provides enough additional data for us to perform a synthesis
109 of 91 unique studies, comprising 9585 individuals, 338 species, 192 genera, and 81 families. In
110 addition, BA presumably better reflects the biomechanical and hydraulic limits for A_L , making
111 this assumption mechanistically consistent with our framework relating $A_L:BA$ to $A_L:A_S$.

112 We performed variance decomposition to determine the taxonomic scales of variation in
113 $A_L:BA$. We used linear mixed effects models for $\log\left(\frac{A_L}{BA}\right)$. First, we built a model including a
114 fixed intercept, fixed effect for method of calculating $A_L:A_S$ (directly from measurements of A_S
115 at DBH or basal height, indirectly from basal diameter or DBH), and nested random effects for
116 family, genus, and species. We compared the size of the random effects’ variance parameters
117 within-species (i.e. residual variance), within-genus, within-family, and between families and
118 found that 50% of the observed variation in $A_L:BA$ across the BAAD database occurred within
119 species (Fig. 1). We then included a fixed effect for $\log(\text{tree height})$ for each plant species
120 (because A_S should theoretically increase more rapidly than A_L with tree height, as resistance to
121 flow increases with tree height). Based on the marginal R^2 of the model with and without the

122 species-level height effect, we determined that roughly 3/5ths of the within-species variation
123 (29% of the total variation in $A_L:BA$) could be attributed to within-species variation related to
124 tree size (Fig. 1, dashed line). Interestingly, within-species patterns of $A_L:BA$ versus height,
125 while negative on average, varied enormously across species, both in strength and direction
126 (Figs. S1-2).

127 The substantial within-species variation, even when controlling for tree size, stands in
128 contrast to numerous other plant functional traits that are often included in vegetation models
129 (Rosas et al., 2019). As an example, we performed an equivalent analysis on wood density
130 (WD), a widely used plant functional trait. We leveraged the huge within-species variation in
131 WD within BAAD combined with cross-species information from the Global Wood Density
132 Database (Zanne et al., 2009). Our synthesis comprised of 217 unique studies, 19997
133 measurements, 8486 species, 1694 genera, and 211 families. In contrast to $A_L:BA$, the majority
134 of the variation in WD occurred at large taxonomic scales (e.g. across plant families, Fig. 1). The
135 strong intraspecific variation that is particularly apparent in $A_L:BA$ indicates that environment
136 strongly influences $A_L:BA$ ($\sim A_L:A_S$), perhaps more so than many common species-specific
137 functional traits. Thus, while allometric functions relating plant size to plant investment in leaves
138 have existed for over half a century and are ubiquitous, the generality and out-of-sample
139 applicability of these functions tends to be low, posing considerable challenges to the
140 formulation of fixed trait-based allocation algorithms in mechanistic vegetation models. This
141 strong intraspecific variation implies that $A_L:A_S$ may need to be predicted from first principles,
142 rather than prescribed as a functional trait.

143

144 **Leaf allocation in mechanistic vegetation models**

145 There are numerous empirical and optimization-based approaches to determining
146 vegetation allocation that often vary with the spatial scope of the model due to computational
147 costs and tradeoffs (Tables 1-3) (De Kauwe et al., 2014; Franklin et al., 2012; Walker et al.,
148 2014). In many vegetation models that run at large spatial scales or over long time periods,
149 vegetation is represented in an aggregated manner analogous to a ‘big leaf’ in each grid cell due
150 to the large computational costs associated with predicting long-term vegetation dynamics across
151 the globe. In this class of vegetation model, allocation often follows an empirical approach where
152 a fixed fraction of net primary productivity (NPP) is allocated to each of leaves, stem, and fine

153 roots (as well as other costs such as reproduction). This includes both models that are coupled to
154 climate models such as the Community Land Model (CLM) family, as well as a number of
155 models that have not been run coupled to climate models and are generally operated at scales
156 smaller than the globe (Tables 1-2).

157 Another class of vegetation model, the ‘individual’- or ‘cohort-based’ model, resolves
158 individual plants. Cohort-based vegetation models generally use allometric scaling functions
159 from the forestry literature that relate model-predicted cohort dbh to tree stem, leaf, and root
160 biomass using fixed relationships (see section on ‘Allometric biomass equations: history/theory’)
161 (Tables 1-2). Thus, NPP partitioning to different tree tissues in cohort-based vegetation models is
162 determined by fixed plant functional type (PFT)-specific parameters and tree size. Though
163 computationally more intensive than the big leaf approach, cohort-based vegetation models are
164 more skilled at capturing competition for light and vegetation demographic processes. Further,
165 significant progress is being made towards incorporating cohort-based vegetation models in the
166 next generation of coupled climate-vegetation models used for global-scale climate change
167 projections (Fisher et al., 2018).

168 Despite the fact that allocation to leaves and other organs in the fixed allocation approach
169 is broadly constrained by PFT-specific fixed coefficients, the fixed coefficient representation of
170 allocation does allow for limited allometric perturbations in response to environment. The
171 representation of phenological processes are one such example of environmental responsiveness.
172 In most fixed allocation vegetation models, deciduous PFTs allocate extra carbon resources to
173 leaves at the beginning of the growing season to meet some target leaf biomass, and cease
174 allocating carbon to leaves at the end of the growing season (though exact allocation fractions
175 are model specific). Phenological responsiveness has been incorporated for both temperate and
176 drought-deciduous ecosystems in a number of vegetation models. The representation of
177 allocation to leaves in CLM4 and CLM5 is another such example, where the ratio of NPP going
178 to leaves relative to stem is a function of previous year’s NPP such that, as vegetation
179 productivity (NPP) increases, more carbon is allocated to wood relative to leaves (Table 2). A
180 third example of environmental responsiveness that is present in numerous fixed allocation
181 models occurs when respiratory costs exceed plant carbon gain. For example, in the Ecosystem
182 Demography (ED) model family, target leaf biomass is fixed based on PFT and dbh. But, when
183 respiration and leaf and root turnover exceed photosynthetic carbon gains, trees cannot allocate

184 to meet target leaf allometries due to environmental stress. Overall, these approaches have begun
185 to incorporate simple environmental feedbacks on plant allometry. However, allocation schemes
186 are generally limited to prescribed tissue ratios that are drawn from the allometric equation
187 literature. Further, allocation is largely rooted in carbon-based allometries, and other ecologically
188 relevant metrics that have been shown to be important in an ecosystem context such as leaf mass
189 per area (Duursma & Falster, 2016; Falster, Duursma, & FitzJohn, 2018) are not often
190 considered.

191 Because plant hydraulic processes are increasingly represented in both big leaf and
192 cohort-based vegetation models that use a fixed allocation approach (see below), it is important
193 to understand how fixed allocation and sub-hourly variations in water stress impact predictions
194 of carbon and energy fluxes. The widespread fixed allocation approach of “growing the same
195 tree everywhere” for a given model PFT is inconsistent with the huge forestry literature on the
196 influence of site-conditions on leaf allocation (Bond-Lamberty et al., 2002; Fayolle et al., 2013;
197 Jenkins et al., 2003; Ketterings et al., 2001; Ter-Mikaelian & Korzukhin, 1997), making it
198 important to consider the impacts on estimates for global terrestrial productivity.

199

200 **The importance of leaf allocation for the physiology of vegetation water stress**

201 Plant allocation to leaves, plant physiological traits, and local environmental conditions
202 interact to affect water supply and demand and determine tree water status, gas exchange, and
203 productivity. While water availability is set by climatic, hydrologic, and edaphic factors, tree
204 water demand is determined in large part by plant morphology and leaf allocation. Water loss
205 through A_L must be matched by water flow through A_S , giving the plant considerable agency
206 over the flow of water through the soil-plant-atmosphere-continuum purely based on its relative
207 allocation to evaporative (A_L) versus solely conductive (A_S) tissue area. Because water stress is
208 the result of unmet plant water demand, allocation to A_L is a major seasonal to multi-annual
209 control over a plant’s exposure to water stress under limiting water supply. Further, water stress
210 has important implications for plant productivity: If no other physiological changes occur, an
211 over allocation of leaves, resulting in a large $A_L:A_S$, will cause stomatal closure to prevent
212 excessive water loss, decrease intercellular CO_2 (C_i), and decrease leaf-level photosynthesis.

213 We illustrate the underlying plant physiological response to A_L -driven changes in water
214 demand with a fixed water supply using a simple tree model (the Hydraulic Optimization Theory

215 for Tree and Ecosystem Resilience or HOTTER model). HOTTER uses a single resistor to
216 represent whole-plant hydraulic transport up to the substomatal cavity and a hydraulic
217 optimization-based stomatal conductance model (Trugman, Detto, et al., 2018; Wolf, Anderegg,
218 & Pacala, 2016) (Fig. 2). While the model contains some necessary simplifications, it is broadly
219 consistent with the Ohm's law analogy for hydraulic elements in series and the observed
220 responses of gas exchange to changes in leaf-specific hydraulic conductance (Hubbard, Ryan,
221 Stiller, & Sperry, 2001; Sperry et al., 2016; Sperry, 2000).

222 As illustrated by the HOTTER model, when a tree increases water demand via increases
223 in A_L , given fixed environmental and physiological conditions, the tree hydraulic conductance
224 (K) per basal area increases to a maximum as more leaves are added and the percent whole tree
225 resistance in leaves declines. Consequently, A_L increases faster than K , leading to a monotonic
226 decline in tree hydraulic conductance per A_L and hence transpiration per A_L . Stomatal closure
227 reduces transpiration per A_L in step with the reduction in hydraulic conductance per A_L , thus
228 maintaining an approximate homeostasis in leaf water potential. The stomatal control on leaf
229 pressure helps avoid the costs of physiological damage due to water stress (Anderegg et al.,
230 2018; Wolf et al., 2016), but drives down leaf-level photosynthesis by limiting C_i (Fig. 2c).
231 Additionally, at higher A_L , self-shading further limits water and carbon fluxes. The reduction in
232 photosynthesis per A_L results in total tree photosynthesis (photosynthesis per leaf times A_L)
233 increasing less rapidly than the linear increase in the cost of leaf canopy construction and
234 maintenance (respiration). Thus, there is an optimal $A_L:A_S$ that maximizes the benefit of
235 increased tree photosynthesis relative to canopy construction and respiratory cost (Fig. 2d-e).
236 Critically, the optimal $A_L:A_S$ is not fixed for a given set of plant hydraulic traits. Rather $A_L:A_S$
237 depends on how local environmental conditions influence the cost-benefit ratio of growing A_L :
238 In drier climate conditions, there are lower carbon benefits, resulting in a lower optimal A_L
239 compared to wetter conditions where a higher A_L is optimal (Westoby, Cornwell, & Falster,
240 2012). Given that trees within an individual species can grow along relatively broad
241 environmental gradients, this can result in significant intraspecific allocational changes to A_L
242 depending on local environmental conditions (L. D. L. Anderegg & HilleRisLambers, 2016;
243 DeLucia, Maherali, & Carey, 2000; Martinez-Vilalta et al., 2009; Mencuccini & Bonosi, 2001;
244 Mencuccini & Grace, 1994; Pinol & Sala, 2000; Rosas et al., 2019), and is likely a driver behind
245 the large intraspecific variation in $A_L:BA$ observed across in the BAAD (Fig. 1).

246 To demonstrate the impact of allocation to leaves on tree level productivity, we used the
247 HOTTER model with input atmospheric vapor pressure deficit (VPD, a metric of atmospheric
248 dryness), soil water content, and atmospheric CO₂ concentration. We ran simulations varying
249 A_L:A_S under two environmental regimes: a drier environment (VPD = 1500 Pa and soil water
250 potential (Ψ_{soil}) = -0.6 MPa) and a wetter environment (VPD = 1000 Pa and Ψ_{soil} = -0.3 MPa).
251 All other traits, tree size, and atmospheric CO₂ were kept constant. In the case where A_L:A_S
252 determined based on the ‘optimal’ A_L:A_S for the wetter environment (i.e., the A_L:A_S that
253 maximized instantaneous tree carbon gain per respiratory and turnover costs given the wetter
254 environment), but the tree was experiencing the drier environment, such as might be the case if
255 the allocation functional relationship were derived from trees in a wet environment and applied
256 to modeling tree allocation in a drier environment, the tree overallocated to A_L by almost twofold
257 relative to the optimum, resulting in a potential ~35% loss of plant carbon gain due to extra
258 respiratory costs and stomatal closure (Fig. 3).

259 Critically, tree-level responses in productivity resulting from A_L:A_S and local
260 environmental conditions significantly affect total ecosystem water fluxes and carbon gain. As
261 an illustrative example of the consequences of fixed allometries in hydraulically enabled models
262 for ecosystem-level carbon predictions, we used site-specific allometry to constrain the leaf
263 allocation strategy of aspen trees growing across a resource gradient between central Alaska and
264 central Canada. We used the ED2 model (Trugman et al., 2016), a cohort-based vegetation
265 model with an explicit representation of plant hydraulic processes designed to run at spatial
266 scales ranging from a flux tower footprint to regional scales (Medvigy, Wofsy, Munger,
267 Hollinger, & Moorcroft, 2009; Medvigy & Moorcroft, 2012). We performed two separate
268 simulations forced with identical climate over a 200-year spin up, but we varied the allometric
269 relationship between dbh and leaf biomass according to two different allometries, one derived
270 from trees sampled in a drier location in central Alaska (Yarie, Kane, & Hall, 2007) and one
271 derived from trees sampled in a wetter location in central Canada (Bond-Lamberty et al., 2002).
272 Depending on the allometric constraints used, ED2 predicted either rapid biomass accumulation
273 within the first 50 years to a stable forest basal area (a metric of forest density) of ~27 cm² m⁻²,
274 compared to a much slower biomass accumulation rate over the multi-century period with a
275 maximum accumulated basal area of 20 cm² m⁻² (~30% lower) at the end of the simulation (Fig.
276 4). While particularly important in models that include plant hydraulics, this central role of

277 allometric equations in influencing carbon pools and fluxes is visible in a wide range of models
278 and ecosystems and has been identified as a major source of model uncertainty in response to
279 elevated CO₂ concentrations (De Kauwe et al., 2014; Walker et al., 2014).

280

281 **Plant hydraulics in mechanistic vegetation models**

282 As illustrated by the HOTTER and ED2 vegetation models above, plant water transport
283 links the carbon costs and benefits of plant allocation strategy. Thus, the representation of water
284 transport in mechanistic models is the scaffolding upon which allometric schemes feedback to
285 influence modeled plant water stress. Many large-scale vegetation models represent the plant
286 physiological response to supply- and demand-driven water stress using two distinct pathways
287 rather than explicitly representing plant hydraulic transport along the soil-plant-atmosphere
288 continuum (see Sperry & Love, (2015), Fatichi (*et al.*, 2016), and Mencuccini *et al.*, (2018) for
289 detailed reviews of the representation of plant water stress and water transport). Physiological
290 responses to supply-driven soil moisture stress are represented in many vegetation models using
291 an empirical factor based on soil moisture and root biomass that down-regulates either
292 photosynthesis or stomatal conductance as soil water decreases below field capacity (Trugman,
293 Medvigy, Mankin, & Anderegg, 2018). Demand-driven water stress responses are represented
294 through an empirical equation that captures the observed relationships between stomatal
295 conductance and environmental drivers, typically humidity or vapor pressure deficit, CO₂
296 concentrations, and photosynthesis (Ball, Woodrow, & Berry, 1987; Leuning, 1995).
297 Importantly, the treatment of supply- and demand-driven limitations as separate pathways
298 influencing water use is unlikely to capture the complex and nonlinear joint influence on
299 stomatal conductance through leaf water potential (Sperry et al., 2017).

300 Vegetation models that do resolve the plant physiological response to water stress use
301 several tissue-level plant hydraulic traits of roots, stems, and leaves, including saturated xylem
302 hydraulic conductivity and the water potential at 50% loss of conductivity. With a resistor-based
303 representation of water transport and a connection between leaf water stress and stomatal
304 conductance (Fig. 2), hydraulically-enabled vegetation models mechanistically link tissue-level
305 stresses to ecosystem-level carbon and water fluxes (Christoffersen et al., 2016; Kennedy et al.,
306 2019; Xu et al., 2016). Coupling of plant hydraulic transport to gas exchange at the stomata can
307 be done either using an empirical function where stomatal conductance is parameterized as a

308 function of leaf water potential, in a manner similar to that of the empirical soil moisture stress
309 function above, or via optimization approaches. A recently-proposed “carbon maximization” or
310 “gain-risk” optimization that explicitly balances the benefit of additional photosynthesis against
311 the risk of hydraulic dysfunction from falling water potentials (Eller et al., 2018; Sperry et al.,
312 2017; Wolf et al., 2016) has yielded predictive improvements of water and carbon fluxes at leaf
313 and whole-tree scales, particularly during drought. This gain-risk approach coupled with tissue-
314 level hydraulic traits to explicitly predict internal plant moisture stress (water potential) exceeds
315 the accuracy of standard empirical models and other optimization approaches (Wang et al. 2019;
316 Anderegg *et al.*, 2018; Venturas *et al.*, 2018), suggesting that optimization approaches based on
317 hydraulic risk provide a rigorous predictive method for improving predictions of carbon, water,
318 and energy fluxes.

319 Despite recent improvements, current state-of-the-art representations of plant hydraulic
320 processes in vegetation models have yet to widely consider how the empirical constraint of fixed
321 allometric traits further affects water relations and productivity. These allometric constraints on
322 $A_L:A_S$ are particularly important when considering that the new representation of plant water
323 relations results in plant water stress varying on sub-hourly scales with leaf water potential (Xu
324 et al., 2016), rather than monthly time scales with soil moisture (Powell et al., 2013; Trugman,
325 Medvigy, et al., 2018). Short temporal variations in water stress impact predictions of sub-hourly
326 carbon fluxes. Thus, because allocation to $A_L:A_S$ is integral in determining leaf-level gas
327 exchange and C_i , a flexible allocation strategy to $A_L:A_S$ that considers local water availability is
328 of critical importance to capturing vegetation dynamics and terrestrial carbon, water, and energy
329 fluxes.

330

331 **Flexible allocation approaches**

332 A number of vegetation models of varying scales have made progress towards allocation
333 strategies that are flexible in response to resource limitation, some even in the context of plant
334 hydraulics. In general, there are two main methodologies for representing flexible allocation in
335 mechanistic models. One method adjusts allocation coefficients depending on the strongest
336 resource limitation. The second type of approach, optimization-based approaches, seek to
337 maximize some proxy of fitness, such as productivity (e.g. Fig. 3) or reproductive success
338 (Farrior, Dybzinski, Levine, & Pacala, 2013) given different key resource limitation axes. Within

339 the two broad categories of flexible allocation approaches, individual vegetation model
340 implementations vary significantly. In this section, we highlight a few key examples of flexible
341 allocation from both resource-seeking and optimization-based models along different limitation
342 axes including light, water, and nutrients. We include further analyses of flexible allocation
343 schemes in Table 3.

344 The Adaptive Dynamic Global Vegetation Model (aDGVM) is one example of a large-
345 scale vegetation model that represents allocation such that tissue biomass partitioning is
346 responsive to environmental conditions. In aDGVM, light-limited trees preferentially allocate to
347 stem (D. A. King, 1994), water limited trees preferentially allocate to roots, and
348 photosynthetically-limited trees preferentially allocate to leaves (Table 3). Flexible allocation is
349 achieved using empirical light- and water-limitation factors based on the relative height of a
350 plant and its surrounding competitors and weighted soil moisture within the rooting zone,
351 respectively (Scheiter & Higgins, 2009). Unstressed allocation (when light and water are not
352 limiting) is defined using fixed coefficients dependent on PFT-specific photosynthetic pathway
353 (e.g. C_3 or C_4).

354 The Terrestrial Regional Ecosystem Exchange Simulator (TREES) is a stand-scale
355 vegetation model that integrates carbon uptake and allocation with plant hydraulic limitations
356 (Table 3). TREES uses the soil-plant water transport model first described in Sperry *et al.*,
357 (1998) and explicitly couples plant hydraulics to photosynthesis and leaf carbon allocation
358 through its leaf turnover function, which relates leaf mortality rate to lateral stem proportional
359 loss of conductivity (Mackay *et al.*, 2015). Given that a fixed amount of total available carbon is
360 allocated to stem, and that leaf turnover rate varies depending on plant hydraulic stress, this
361 allocation scheme decreases A_L from a predetermined initial value that is dependent on site-
362 specific allometries in response to hydraulic impairment. Using this leaf turnover scheme that is
363 responsive to hydraulic stress, TREES was able to accurately capture A_L dynamics and species-
364 specific differences in semi-arid piñon pine and juniper forests in the southwestern United States
365 (Mackay *et al.*, 2015).

366 Though computationally more intensive, optimization-based approaches that account for
367 both the morphological and physiological facets of plant above- and below-ground allocation
368 responses to resource stress provide a promising alternative to fixed allometric approaches
369 because the optimization allows for allocation to be predicted from plant functional traits and

370 environment (Sperry et al., 2012). In the context of light limitation, the Community Land Model
371 Functionally Assembled Terrestrial Ecosystem Simulator (CLM-FATES) model utilizes an
372 annualized optimization-based “trimming” factor that allows for removal of leaves in negative
373 carbon balance within the canopy if the annual maintenance cost of the lowest leaf layer is less
374 than the carbon gain (Lawrence et al., 2018). This trimming approach is present in a number of
375 vegetation models (Table 3).

376 In the context of water limitation, Magnani, Mencuccini, & Grace, (2000) developed one
377 of the first tree-level models that integrates plant hydraulics to test the hypothesis that age-related
378 declines in forest productivity are driven by allocational shifts to leaves, stem, and fine roots
379 associated with tree height changes. In their model, Magnani, Mencuccini, & Grace, (2000)
380 optimize allocation of carbon to conductive sapwood and absorbing root tissues to minimize
381 whole-plant leaf-specific hydraulic resistance while maximizing leaf-tissue. Thus, to avoid
382 negative water potentials as a tree grows taller, plant allocation shifts from leaves to transport
383 tissues because resistance to water transport through the tree stem is proportional to tree height,
384 so transport tissue must increase more rapidly than leaf tissue with height. This size-dependent
385 allocation scheme based on plant hydraulic constraints has been implemented in a version of
386 Lund–Potsdam–Jena (LPJ) vegetation model (Hickler, Prentice, Smith, Sykes, & Zaehle, 2006;
387 Zaehle et al., 2006) (Table 3). A number of other optimization studies have used the concept of
388 ecohydrological equilibrium, where allocation to leaves and roots is assumed to be in equilibrium
389 with water availability (Eagleson, 1982; Westoby et al., 2012). The ecohydrological equilibrium
390 framework has successfully reproduced observed trends in A_L and root distributions across
391 environmental gradients (Cabon, Martínez-Vilalta, Martínez de Aragón, Poyatos, & De Cáceres,
392 2018; Schymanski, Sivapalan, Roderick, Beringer, & Hutley, 2008; Yang, Medlyn, De Kauwe,
393 & Duursma, 2018).

394 Further, optimization approaches that account for multiple resource limitations have
395 been implemented, particularly in the context of nutrient and light limitation (Dewar, Franklin,
396 Mäkelä, McMurtrie, & Valentine, 2009; Rastetter & Shaver, 1992). For example, in the simple
397 vegetation model ACONITE (Analyze Carbon and Nitrogen Interactions in Terrestrial
398 Ecosystems), Thomas & Williams, (2014) account for the productivity tradeoffs associated with
399 allocating carbon and nitrogen to different tissues (Table 3). The ACONITE allocation scheme is
400 executed through a relatively complex multi-timescale optimization: At each daily time step,

401 instantaneous carbon return is calculated to determine whether investing further carbon and
402 nitrogen in foliage will result in a positive carbon net uptake (up to some maximum leaf carbon
403 which is set on an annual timescale). If the maximum leaf allocation has been reached or
404 nitrogen limits further leaf allocation, carbon is allocated to fill storage, grow wood, or increase
405 fine roots. Further surplus carbon is allocated for nitrogen fixation. At the end of each annual
406 cycle, integrated annual marginal carbon return is used to recompute maximum leaf carbon and
407 nitrogen and maximum root carbon and nitrogen. Thus, at each timestep, ACONITE computes
408 the marginal changes to photosynthesis from added leaf carbon, added leaf nitrogen, and added
409 leaf carbon and nitrogen together, to determine an appropriate allocation strategy.

410

411 **Frontiers in allocation prediction**

412 In this section, we expand the understanding of allocation drawn from the vegetation
413 hydraulic framework to comment broadly on the global optimization problem of allocation to
414 plant tissues in the presence of multiple resource constraints. Specifically, we highlight current
415 questions arising from flexible allocation schemes, including limitations of both resource-
416 seeking approaches and optimization-based approaches. Concomitantly, we suggest several ways
417 forward to improve the representation of allocation in vegetation models.

418 Current resource-seeking implementations of flexible allocation still face challenges
419 associated with (a) quantifying the degree and costs of light, water, and nutrient limitation, and
420 (b) uncertainty associated with physiological parameters such as root hydraulic resistance, which
421 can be treated as model calibration factors rather than an observationally-constrained biological
422 traits. As a result, a number of vegetation models with resource-seeking allocation effectively
423 trade empirical allometric allocation factors (based on site-specific, but field-measured
424 allometric relationships) for empirical cost factors that may be loosely rooted in limitation
425 mechanisms, such as soil water/nutrient availability or relative tree height of competitors (Table
426 3). Such tradeoffs should be undertaken with caution because the empirical cost factors are
427 difficult to validate using field measurements and are unlikely to capture any nonlinear changes
428 in allocation responses to resource scarcity, as might be expected in out of sample environmental
429 conditions. Further, most resource-limitation schemes still rely on fixed coefficients to define
430 allocational strategies under unstressed conditions (Krinner et al., 2005; Lawrence et al., 2018;
431 Mackay et al., 2015; Scheiter & Higgins, 2009).

432 Key challenges to address in advancing flexible allocational schemes in vegetation
433 models will be to: (1) limit additional free parameters, (2) tie the mechanisms underlying flexible
434 allocation to known aspects of plant physiology such as plant functional traits, (3) assess whether
435 any increases in model complexity towards a more physiological accurate representation of
436 biomass allocation are justified based on model performance. In particular, the universal problem
437 of equifinality (many parameter choices yielding similar model behavior) in vegetation models
438 with many unconstrained or poorly constrained parameters emphasizes the need to implement
439 parsimonious allocation schemes driven by parameters that can be constrained by observations
440 (Tang & Zhuang, 2008). Otherwise, flexible allocation schemes may fit training data well yet not
441 beat simplistic but empirically constrained fixed allocation schemes when considering multiple
442 measures of model prediction skill.

443 Recent advances in the field of plant hydraulics provide several examples of methods to
444 mechanistically quantify costs of scarce resource limitation that are informative to the flexible
445 allocation problem. For example, Mackay *et al.*, (2015) accelerated leaf shedding in response to
446 water limitation as a function of lateral stem proportional loss of conductivity and Sperry *et al.*,
447 (2017) defined a hydraulic damage risk function based on the fractional loss of plant hydraulic
448 conductance. Though these approaches are not fully mechanistic, they offer potential
449 improvements that connect hydraulic mechanisms to allocation and damage costs experienced by
450 plants. Additionally, the cost functions associated with hydraulic conductivity or conductance
451 have performed well when tested against diverse allocational and physiological observational
452 datasets (Eller *et al.*, 2018; Mackay *et al.*, 2015; Sperry *et al.*, 2017; Venturas *et al.*, 2018).

453 Optimality approaches show significant promise for predicting the interaction between
454 plant biophysics and environment and have been implemented in the context of plant hydraulics,
455 as illustrated by the HOTTER model example (Trugman *et al.*, 2019), and for multiple resource
456 limitations (i.e. Rastetter & Shaver, 1992; Farrior *et al.*, 2013; Thomas & Williams, 2014;
457 Dybzinski *et al.*, 2015) in simple models. However, the calculation of the marginal costs and
458 benefits associated with allocation tradeoffs can be extremely computationally expensive.
459 Further, the implementation of optimized allocation brings up a number of plant physiological
460 questions that are currently unknown (Dewar *et al.*, 2009). Particularly, how rapidly can plants
461 adjust allocation? How does environmental variability factor into plant allocation strategy? How
462 does competition impact allocation strategy (i.e. Falster & Westoby, 2003; Farrior *et al.*, 2013;

463 Dybzinski *et al.*, 2015)? How do plants reconcile short-term and long-term tradeoffs such as
464 sacrificing height-growth, which increases short-term carbon gain but ultimately leads to a long-
465 term competitive disadvantage (Buckley & Roberts, 2006; D. King, 1981)?

466 Given the significant advantages of optimality principles, but substantial computational
467 tradeoffs, hybrid approaches that utilize carbon-balance optimization techniques to define
468 resource cost functions associated with allocation to different tissues under varying resource
469 constraints could prove to be computationally more feasible and avoid drawbacks associated
470 with determining the appropriate optimization timescale. For example, allocation routines could
471 calculate marginal changes in plant fitness (such as carbon gain) in response to increased
472 allocation to leaf, root, and stem tissue given a fixed resource availability, similar to the size-
473 based approach in (Zaehle *et al.*, 2006), as illustrated in Fig. 5.

474

475 **Conclusions**

476 Overall, we now have the tools to tackle allocation broadly in the presence of multiple
477 limiting resources. In particular, cohort-based vegetation models allow us to tackle the impacts
478 of light limitation on allocation (Fisher *et al.*, 2018; Lawrence *et al.*, 2018). Vegetation models
479 that incorporate plant hydraulics (Christoffersen *et al.*, 2016; Kennedy *et al.*, 2019; Xu *et al.*,
480 2016) give us an increased ability to understand how water limitation impacts allocation. Models
481 that include microbe-mediated biogeochemistry and competition for nitrogen and phosphorus
482 allow us to predict nutrient limitations on allocation and growth (Medvigy *et al.*, 2019). Though
483 these connections are not yet fully realized, they represent a promising area of future
484 development.

485

486 **Acknowledgements**

487 A.T.T. acknowledges support from the USDA National Institute of Food and Agriculture
488 Postdoctoral Research Fellowship Grant No. 2018-67012-28020. W.R.L.A was supported by the
489 David and Lucille Packard Foundation, National Science Foundation grants 1714972 and
490 1802880, and the USDA National Institute of Food and Agriculture, Agricultural and Food
491 Research Initiative Competitive Programme, Ecosystem Services and Agro-ecosystem
492 Management, grant no. 2018-67019-27850. L.D.L.A was supported by the National Science

493 Foundation (DBI-1711243) and the National Oceanic and Atmospheric Administration (Climate
494 and Global Change Fellowship).

495 **References**

496 Anderegg, L. D. L., & HilleRisLambers, J. (2016). Drought stress limits the geographic ranges of
497 two tree species via different physiological mechanisms. *Global Change Biology*, *22*(3),
498 1029–1045. <https://doi.org/10.1111/gcb.13148>

499 Anderegg, W. R. L., Wolf, A., Arango-velez, A., Choat, B., Chmura, D. J., Jansen, S., ... Pacala,
500 S. W. (2018). Woody plants optimise stomatal behaviour relative to hydraulic risk. *Ecology*
501 *Letters*. <https://doi.org/10.1111/ele.12962>

502 Ball, J. T., Woodrow, I. E., & Berry, J. A. (1987). A Model Predicting Stomatal Conductance
503 and its Contribution to the Control of Photosynthesis under Different Environmental
504 Conditions. In J. Biggins (Ed.), *Progress in Photosynthesis, ed Biggins J (Springer,*
505 *Dordrecht, The Netherlands)* (pp. 221–224). Dordrecht: Springer Netherlands.
506 https://doi.org/10.1007/978-94-017-0519-6_48

507 Bartlett, M. K., Scoffoni, C., & Sack, L. (2012). The determinants of leaf turgor loss point and
508 prediction of drought tolerance of species and biomes: a global meta-analysis. *Ecology*
509 *Letters*, *15*(5), 393–405. <https://doi.org/10.1111/j.1461-0248.2012.01751.x>

510 Baskerville, G. L. (1972). New titin isoforms in skeletal muscles of mammals. *Canadian Journal*
511 *of Forestry*, *2*(49). <https://doi.org/10.1023/B:DOBI.0000025559.14249.43>

512 Bonan, G. (2008). Forests and Climate Change: Forcings, Feedbacks, and the Climate Benefits
513 of Forests. *Science*, *320*, 1444–1449.

514 Bond-Lamberty, B., Wang, C., & Gower, S. T. (2002). Aboveground and belowground biomass
515 and sapwood area allometric equations for six boreal tree species of northern Manitoba.
516 *Canadian Journal of Forest Research*, *32*(8), 1441–1450. <https://doi.org/10.1139/x02-063>

517 Buckley, T. N., & Roberts, D. W. (2006). DESPOT, a process-based tree growth model that
518 allocates carbon to maximize carbon gain. *Tree Physiology*, *26*(2), 129–144. Retrieved from
519 <http://www.ncbi.nlm.nih.gov/pubmed/16356910>

520 Cabon, A., Martínez-Vilalta, J., Martínez de Aragón, J., Poyatos, R., & De Cáceres, M. (2018).
521 Applying the eco-hydrological equilibrium hypothesis to model root distribution in water-
522 limited forests. *Ecohydrology*, (July), 1–16. <https://doi.org/10.1002/eco.2015>

523 Chave, J., Condit, R., Aguilar, S., Hernandez, A., Lao, S., & Perez, R. (2004). Error propagation

524 and sealing for tropical forest biomass estimates. *Philosophical Transactions of the Royal*
525 *Society B: Biological Sciences*, 359(1443), 409–420. <https://doi.org/10.1098/rstb.2003.1425>

526 Chave, J., Réjou-Méchain, M., Búrquez, A., Chidumayo, E., Colgan, M. S., Delitti, W. B. C., ...
527 Vieilledent, G. (2014). Improved allometric models to estimate the aboveground biomass of
528 tropical trees. *Global Change Biology*, 20(10), 3177–3190.
529 <https://doi.org/10.1111/gcb.12629>

530 Choat, B., Jansen, S., Brodribb, T. J., Cochard, H., Delzon, S., Bhaskar, R., ... Zanne, A. E.
531 (2012). Global convergence in the vulnerability of forests to drought. *Nature*, 491(7426),
532 752–755. <https://doi.org/10.1038/nature11688>

533 Christoffersen, B. O., Gloor, M., Fauset, S., Fyllas, N. M., Galbraith, D. R., Baker, T. R., ...
534 Meir, P. (2016). Linking hydraulic traits to tropical forest function in a size-structured and
535 trait-driven model (TFS v.1-Hydro). *Geoscientific Model Development*, 9(11), 4227–4255.
536 <https://doi.org/10.5194/gmd-9-4227-2016>

537 De Kauwe, M. G., Medlyn, B. E., Zaehle, S., Walker, A. P., Dietze, M. C., Wang, Y. P., ...
538 Norby, R. J. (2014). Where does the carbon go? A model-data intercomparison of
539 vegetation carbon allocation and turnover processes at two temperate forest free-air
540 CO₂ enrichment sites. *New Phytologist*, 203(3), 883–899. <https://doi.org/10.1111/nph.12847>

541 DeLucia, E. H., Maherali, H., & Carey, E. V. (2000). Climate-driven changes in biomass
542 allocation in pines. *Global Change Biology*, 6(5), 587–593. <https://doi.org/10.1046/j.1365-2486.2000.00338.x>

544 Dewar, R. C., Franklin, O., Mäkelä, A., McMurtrie, R. E., & Valentine, H. T. (2009). Optimal
545 Function Explains Forest Responses to Global Change. *BioScience*, 59(2), 127–139.
546 <https://doi.org/10.1525/bio.2009.59.2.6>

547 Duursma, R. A., & Falster, D. S. (2016). Leaf mass per area, not total leaf area, drives
548 differences in above-ground biomass distribution among woody plant functional types. *The*
549 *New Phytologist*, 212(2), 368–376. <https://doi.org/10.1111/nph.14033>

550 Dybzinski, R., Farris, C. E., & Pacala, S. W. (2015). Increased forest carbon storage with
551 increased atmospheric CO₂ despite nitrogen limitation: A game-theoretic allocation model
552 for trees in competition for nitrogen and light. *Global Change Biology*, 21(3), 1182–1196.
553 <https://doi.org/10.1111/gcb.12783>

554 Eagleson, P. S. (1982). Ecological optimality in water-limited natural soil-vegetation systems: 1.

555 Theory and hypothesis. *Water Resources Research*, 18(2), 325–340.
556 <https://doi.org/10.1029/WR018i002p00325>

557 Eller, C. B., Rowland, L., Oliveira, R. S., Bittencourt, P. R. L., Barros, F. V., da Costa, A. C. L.,
558 ... Cox, P. (2018). Modelling tropical forest responses to drought and El Niño with a
559 stomatal optimization model based on xylem hydraulics. *Philosophical Transactions of the*
560 *Royal Society B: Biological Sciences*, 373(1760), 20170315.
561 <https://doi.org/10.1098/rstb.2017.0315>

562 Falster, D. S., Duursma, R. A., & FitzJohn, R. G. (2018). How functional traits influence plant
563 growth and shade tolerance across the life cycle. *Proceedings of the National Academy of*
564 *Sciences*, 115(29), E6789–E6798. <https://doi.org/10.1073/pnas.1714044115>

565 Falster, D. S., Duursma, R. A., Ishihara, M. I., Barneche, D. R., FitzJohn, R. G., Vårhammar, A.,
566 ... York, R. A. (2015). BAAD: a Biomass And Allometry Database for woody plants.
567 *Ecology*, 96(5), 1445. <https://doi.org/10.1890/14-1889.1>

568 Falster, D. S., & Westoby, M. (2003). Plant height and evolutionary games. *Trends in Ecology*
569 *and Evolution*, 18(7), 337–343. [https://doi.org/10.1016/S0169-5347\(03\)00061-2](https://doi.org/10.1016/S0169-5347(03)00061-2)

570 Fariior, C. E., Dyzinski, R., Levine, S. A., & Pacala, S. W. (2013). Competition for Water and
571 Light in Closed-Canopy Forests: A Tractable Model of Carbon Allocation with Implications
572 for Carbon Sinks. *The American Naturalist*, 181(3). <https://doi.org/10.1086/669153>

573 Fatichi, S., Pappas, C., & Ivanov, V. Y. (2016). Modeling plant-water interactions: an
574 ecohydrological overview from the cell to the global scale. *Wiley Interdisciplinary Reviews:*
575 *Water*, 3(3), 327–368. <https://doi.org/10.1002/wat2.1125>

576 Fayolle, A., Doucet, J. L., Gillet, J. F., Bourland, N., & Lejeune, P. (2013). Tree allometry in
577 Central Africa: Testing the validity of pantropical multi-species allometric equations for
578 estimating biomass and carbon stocks. *Forest Ecology and Management*, 305, 29–37.
579 <https://doi.org/10.1016/j.foreco.2013.05.036>

580 Fisher, R. A., Koven, C. D., Anderegg, W. R. L., Christoffersen, B. O., Dietze, M. C., Fariior, C.
581 E., ... Moorcroft, P. R. (2018). Vegetation demographics in Earth System Models: A review
582 of progress and priorities. *Global Change Biology*, 24(1), 35–54.
583 <https://doi.org/10.1111/gcb.13910>

584 Franklin, O., Johansson, J., Dewar, R. C., Dieckmann, U., McMurtrie, R. E., Brännström, A. K.,
585 & Dyzinski, R. (2012). Modeling carbon allocation in trees: A search for principles. *Tree*

586 *Physiology*, 32(6), 648–666. <https://doi.org/10.1093/treephys/tpr138>

587 Friedlingstein, P., Joel, G., Field, C. B., & Fung, I. Y. (1999). Toward an allocation scheme for
588 global terrestrial carbon models. *Global Change Biology*, 5, 755–770.
589 <https://doi.org/10.1046/j.1365-2486.1999.00269.x>

590 Friend, A. D., Stevens, A. K., Knox, R. G., & Cannell, M. G. R. (1997). A process-based,
591 terrestrial biosphere model of ecosystem dynamics (Hybrid v3.0). *Ecological Modelling*,
592 95(2–3), 249–287. [https://doi.org/10.1016/S0304-3800\(96\)00034-8](https://doi.org/10.1016/S0304-3800(96)00034-8)

593 Hickler, T., Prentice, I. C., Smith, B., Sykes, M. T., & Zaehle, S. (2006). Implementing plant
594 hydraulic architecture within the LPJ Dynamic Global Vegetation Model. *Global Ecology*
595 *and Biogeography*, 0(0), 060811081017001-??? [https://doi.org/10.1111/j.1466-](https://doi.org/10.1111/j.1466-822X.2006.00254.x)
596 [822X.2006.00254.x](https://doi.org/10.1111/j.1466-822X.2006.00254.x)

597 Hubbard, R. M., Ryan, M. G., Stiller, V., & Sperry, J. S. (2001). Stomatal conductance and
598 photosynthesis vary linearly with plant hydraulic conductance in ponderosa pine. *Plant,*
599 *Cell and Environment*, 24, 113–121.

600 Jenkins, J. C., Chojnacky, D. C., Heath, L. S., & Birdsey, R. A. (2003). National-scale biomass
601 estimators for United States tree species. *Forest Science*, 49(1), 12–35.
602 <https://doi.org/10.2737/NE-GTR-310>

603 Kennedy, D., Swenson, S., Oleson, K. W., Lawrence, D. M., Fisher, R. A., da Costa, A. C. L., &
604 Gentine, P. (2019). Implementing plant hydraulics in the Community Land Model, version
605 5. *Journal of Advances in Modeling Earth Systems*, 1–29.
606 <https://doi.org/10.1029/2018ms001500>

607 Ketterings, Q. M., Coe, R., Van Noordwijk, M., Ambagau, Y., & Palm, C. A. (2001). Reducing
608 uncertain in the use of allometric biomass equation for predicting above-ground tree
609 biomass in mixed secondary forests. *Forest Ecology and Management*, 146, 199–209.
610 [https://doi.org/Reducing uncertain in the use of allometric biomass equation for predicting](https://doi.org/Reducing%20uncertain%20in%20the%20use%20of%20allometric%20biomass%20equation%20for%20predicting%20above-ground%20tree%20biomass%20in%20mixed%20secondary%20forests)
611 [above-ground tree biomass in mixed secondary forests](https://doi.org/Reducing%20uncertain%20in%20the%20use%20of%20allometric%20biomass%20equation%20for%20predicting%20above-ground%20tree%20biomass%20in%20mixed%20secondary%20forests)

612 King, D. (1981). Tree dimensions: Maximizing the rate of height growth in dense stands.
613 *Oecologia*, 51(3), 351–356. <https://doi.org/10.1007/BF00540905>

614 King, D. A. (1994). Influence of light level on the growth and morphology of saplings in a
615 Panamanian forest. *American Journal of Botany*, 81(8), 948–957.

616 Krinner, G., Viovy, N., de Noblet-Ducoudré, N., Ogée, J., Polcher, J., Friedlingstein, P., ...

617 Prentice, I. C. (2005). A dynamic global vegetation model for studies of the coupled
618 atmosphere-biosphere system. *Global Biogeochemical Cycles*, 19(1).
619 <https://doi.org/10.1029/2003gb002199>

620 Lawrence, D., Fisher, R., Koven, C., Oleson, K., Swenson, S., & Vertenstein, M. (2018). CLM5
621 Technical Note. *The National Center for Atmospheric Research*.

622 Leuning, R. (1995). A critical appraisal of combined stomatal-photosynthesis model for C3
623 plants. *Plant, Cell and Environment*, 18, 339–355.

624 Lines, E. R., Zavala, M. A., Purves, D. W., & Coomes, D. A. (2012). Predictable changes in
625 aboveground allometry of trees along gradients of temperature, aridity and competition.
626 *Global Ecology and Biogeography*, 21(10), 1017–1028. [https://doi.org/10.1111/j.1466-
627 8238.2011.00746.x](https://doi.org/10.1111/j.1466-8238.2011.00746.x)

628 Mackay, D. S., Roberts, D. E., Ewers, B. E., Sperry, J. S., McDowell, N. G., & Pockman, W. T.
629 (2015). Interdependence of chronic hydraulic dysfunction and canopy processes can
630 improve integrated models of tree response to drought. *Water Resources Research*, (51),
631 6156–6176. <https://doi.org/10.1002/2015WR017244>

632 Magnani, F., Mencuccini, M., & Grace, J. (2000). Age-related decline in stand productivity: The
633 role of structural acclimation under hydraulic constraints. *Plant, Cell and Environment*,
634 23(3), 251–263. <https://doi.org/10.1046/j.1365-3040.2000.00537.x>

635 Martinez-Vilalta, J., Cochard, H., Mencuccini, M., Sterck, F., Herrero, A., Korhonen, J. F. J., ...
636 Zweifel, R. (2009). Hydraulic adjustment of Scots pine across Europe. *New Phytologist*,
637 184, 353–364.

638 Medvigy, D., Wofsy, S. C., Munger, J. W., Hollinger, D. Y., & Moorcroft, P. R. (2009).
639 Mechanistic scaling of ecosystem function and dynamics in space and time: Ecosystem
640 Demography model version 2. *Journal of Geophysical Research*, 114(G1), G01002.
641 <https://doi.org/10.1029/2008JG000812>

642 Medvigy, David, & Moorcroft, P. R. (2012). Predicting ecosystem dynamics at regional scales:
643 an evaluation of a terrestrial biosphere model for the forests of northeastern North America.
644 *Philosophical Transactions of the Royal Society of London. Series B, Biological Sciences*,
645 367(1586), 222–235. <https://doi.org/10.1098/rstb.2011.0253>

646 Medvigy, David, Wang, G., Zhu, Q., Riley, W. J., Trierweiler, A. M., Waring, B. G., ... Powers,
647 J. S. (2019). Observed variation in soil properties can drive large variation in modeled forest

648 functioning and composition during tropical forest secondary succession. *New Phytologist*,
649 nph.15848. <https://doi.org/10.1111/nph.15848>

650 Mencuccini, M., & Bonosi, L. (2001). Leaf/sapwood area ratios in Scots pine show acclimation
651 across Europe. *Canadian Journal of Forest Research*, 31(3), 442–456.
652 <https://doi.org/10.1139/x00-173>

653 Mencuccini, M., & Grace, J. (1994). Climate Influences the Leaf Area/Sapwood Area in Scots
654 Pine. *Tree Physiology*, 15(2), 1–10.

655 Mencuccini, M., Manzoni, S., & Christoffersen, B. O. (2018). Modelling water fluxes in plants:
656 from tissues to biosphere and back. *New Phytologist*, (1991), 1–24.
657 <https://doi.org/10.1111/nph.15681>

658 Oleson, K. W., Lawrence, D. M., Bonan, G. B., Flanner, M. G., Kluzek, E., Lawrence, P. J., ...
659 Thornton, P. E. (2010). Technical Description of version 4.0 of the Community Land Model
660 (CLM). *NCAR Technical Notes*, TN-478, 1–257.

661 Pan, Y., Birdsey, R. A., Fang, J., Houghton, R., Kauppi, P. E., Kurz, W. A., ... Hayes, D. (2011).
662 A Large and Persistent Carbon Sink in the World's Forests. *Science*.

663 Pavlick, R., Drewry, D. T., Bohn, K., Reu, B., & Kleidon, A. (2013). The Jena Diversity-
664 Dynamic Global Vegetation Model (JeDi-DGVM): a diverse approach to representing
665 terrestrial biogeography and biogeochemistry based on plant functional trade-offs.
666 *Biogeosciences*, 10(6), 4137–4177. <https://doi.org/10.5194/bg-10-4137-2013>

667 Pinol, J., & Sala, A. (2000). Ecological Implications of Xylem Cavitation for Several Pinaceae in
668 the Pacific Northern USA. *Functional Ecology*, 14(5), 538–545.

669 Ploton, P., Barbier, N., Momo, S. T., Rejou-Mechain, M., Boyemba Bosela, F., Chuyong, G., ...
670 Pélissier, R. (2016). Closing a gap in tropical forest biomass estimation: Taking crown mass
671 variation into account in pantropical allometries. *Biogeosciences*, 13(5), 1571–1585.
672 <https://doi.org/10.5194/bg-13-1571-2016>

673 Powell, T. L., Galbraith, D. R., Christoffersen, B. O., Harper, A., Imbuzeiro, H. M., Rowland, L.,
674 ... Moorcroft, P. R. (2013). Confronting model predictions of carbon fluxes with
675 measurements of Amazon forests subjected to experimental drought. *New Phytol*, 200(2),
676 350–365. <https://doi.org/10.1111/nph.12390>

677 Rastetter, E. B., & Shaver, G. R. (1992). A Model of Multiple-Element Limitation for
678 Acclimating Vegetation. *Ecology*, 73(4), 1157–1174.

- 679 Rosas, T., Mencuccini, M., Barba, J., Cochard, H., Saura-Mas, S., & Martínez-Vilalta, J. (2019).
680 *Adjustments and coordination of hydraulic, leaf and stem traits along a water availability*
681 *gradient. New Phytologist*. <https://doi.org/10.1111/nph.15684>
- 682 Sato, H., Itoh, A., & Kohyama, T. (2007). SEIB–DGVM: A new Dynamic Global Vegetation
683 Model using a spatially explicit individual-based approach. *Ecological Modelling*, 200(3–
684 4), 279–307. <https://doi.org/10.1016/j.ecolmodel.2006.09.006>
- 685 Scheiter, S., & Higgins, S. I. (2009). Impacts of climate change on the vegetation of Africa: an
686 adaptive dynamic vegetation modelling approach. *Glob Chang Biol*, 15(9), 2224–2246.
687 <https://doi.org/10.1111/j.1365-2486.2008.01838.x>
- 688 Schymanski, S. J., Sivapalan, M., Roderick, M. L., Beringer, J., & Hutley, L. B. (2008). An
689 optimality-based model of the coupled soil moisture and root dynamics. *Hydrology and*
690 *Earth System Sciences*, 12, 913–932.
- 691 Sitch, S., Smith, B., Prentice, I. C., Arneth, A., Bondeau, A., Cramer, W., ... Venevsky, S.
692 (2003). Evaluation of ecosystem dynamics, plant geography and terrestrial carbon cycling
693 in the LPJ dynamic global vegetation model. *Glob Chang Biol*, 9(2), 161–185.
694 <https://doi.org/10.1046/j.1365-2486.2003.00569.x>
- 695 Sperry, J S, Adler, F. R., Campbell, G. S., & Comstock, J. P. (1998). Limitation of plant water
696 use by rhizosphere and xylem conductance: results from a model. *Plant, Cell and*
697 *Environment*, 21, 347–359.
- 698 Sperry, J S, & Love, D. M. (2015). What plant hydraulics can tell us about responses to climate-
699 change droughts. *New Phytologist*, 207(1), 14–27. <https://doi.org/10.1111/nph.13354>
- 700 Sperry, J S, Wang, Y., Wolfe, B. T., Mackay, D. S., Anderegg, W. R., McDowell, N. G., &
701 Pockman, W. T. (2016). Pragmatic hydraulic theory predicts stomatal responses to climatic
702 water deficits. *New Phytol*. <https://doi.org/10.1111/nph.14059>
- 703 Sperry, John S. (2000). Hydraulic constraints on plant gas exchange. *Agricultural and Forest*
704 *Meteorology*, 104(1), 13–23. [https://doi.org/10.1016/S0168-1923\(00\)00144-1](https://doi.org/10.1016/S0168-1923(00)00144-1)
- 705 Sperry, John S., Smith, D. D., Savage, V. M., Enquist, B. J., McCulloh, K. A., Reich, P. B., ...
706 von Allmen, E. I. (2012). A species-level model for metabolic scaling in trees I. Exploring
707 boundaries to scaling space within and across species. *Functional Ecology*, 26(5), 1054–
708 1065. <https://doi.org/10.1111/j.1365-2435.2012.02022.x>
- 709 Sperry, John S., Venturas, M. D., Anderegg, W. R. L., Mencuccini, M., Mackay, D. S., Wang,

- 710 Y., & Love, D. M. (2017). Predicting stomatal responses to the environment from the
711 optimization of photosynthetic gain and hydraulic cost. *Plant Cell and Environment*, 40(6),
712 816–830. <https://doi.org/10.1111/pce.12852>
- 713 Tang, J., & Zhuang, Q. (2008). Equifinality in parameterization of process-based
714 biogeochemistry models: A significant uncertainty source to the estimation of regional
715 carbon dynamics. *Journal of Geophysical Research: Biogeosciences*, 113(4), 1–13.
716 <https://doi.org/10.1029/2008JG000757>
- 717 Ter-Mikaelian, M. T., & Korzukhin, M. D. (1997). Biomass equations for sixty five North
718 American tree species. *Forest Ecology and Management*, 97, 1–24.
- 719 Thomas, R. Q., & Williams, M. (2014). A model using marginal efficiency of investment to
720 analyze carbon and nitrogen interactions in terrestrial ecosystems (ACONITE Version 1).
721 *Geoscientific Model Development*, 7(5), 2015–2037. [https://doi.org/10.5194/gmd-7-2015-](https://doi.org/10.5194/gmd-7-2015-2014)
722 2014
- 723 Trugman, A., Anderegg, L., Wolfe, B., Birami, B., Ruehr, N., Detto, M., ... Anderegg, W.
724 (2019). Climate and plant trait strategies determine tree carbon allocation to leaves and
725 mediate future forest productivity. *Global Change Biology*.
- 726 Trugman, A. T., Detto, M., Bartlett, M. K., Medvigy, D., Anderegg, W. R. L., Schwalm, C., ...
727 Pacala, S. W. (2018). Tree carbon allocation explains forest drought-kill and recovery
728 patterns. *Ecology Letters*. <https://doi.org/10.1111/ele.13136>
- 729 Trugman, A. T., Fenton, N. J., Bergeron, Y., Xu, X., Welp, L. R., & Medvigy, D. (2016).
730 Climate, soil organic layer, and nitrogen jointly drive forest development after fire in the
731 North American boreal zone. *Journal of Advances in Modeling Earth Systems*, 8(3), 1180–
732 1209. <https://doi.org/10.1002/>
- 733 Trugman, A. T., Medvigy, D., Mankin, J. S., & Anderegg, W. R. L. (2018). Soil Moisture Stress
734 as a Major Driver of Carbon Cycle Uncertainty. *Geophysical Research Letters*, (Yang),
735 6495–6503. <https://doi.org/10.1029/2018GL078131>
- 736 Venturas, M. D., Sperry, J. S., Love, D. M., Frehner, E. H., Allred, M. G., Wang, Y., &
737 Anderegg, W. R. L. (2018). A stomatal control model based on optimization of carbon gain
738 versus hydraulic risk predicts aspen sapling responses to drought. *New Phytologist*.
739 <https://doi.org/10.1111/nph.15333>
- 740 Walker, A. P., Hanson, P. J., De Kauwe, M. G., Medlyn, B. E., Zaehle, S., Asao, S., ... Norby,

741 R. J. (2014). Comprehensive ecosystem model-data synthesis using multiple data sets at two
742 temperate forest free-air CO₂ enrichment experiments: Model performance at ambient CO₂
743 concentration. *Journal of Geophysical Research: Biogeosciences*.
744 <https://doi.org/10.1002/2013JG002516>. Received

745 Wang, Y. P., Kowalczyk, E., Leuning, R., Abramowitz, G., Raupach, M. R., Pak, B., ... Luhar,
746 A. (2011). Diagnosing errors in a land surface model (CABLE) in the time and frequency
747 domains. *Journal of Geophysical Research: Biogeosciences*, *116*(1), 1–18.
748 <https://doi.org/10.1029/2010JG001385>

749 Weng, E. S., Malyshev, S., Lichstein, J. W., Farrior, C. E., Dybzinski, R., Zhang, T., ... Pacala,
750 S. W. (2015). Scaling from individual trees to forests in an Earth system modeling
751 framework using a mathematically tractable model of height-structured competition.
752 *Biogeosciences*, *12*(9), 2655–2694. <https://doi.org/10.5194/bg-12-2655-2015>

753 Westoby, M., Cornwell, W. K., & Falster, D. S. (2012). An evolutionary attractor model for
754 sapwood cross section in relation to leaf area. *Journal of Theoretical Biology*, *303*, 98–109.
755 <https://doi.org/10.1016/j.jtbi.2012.03.008>

756 Whittaker, R. H., & Woodwell, G. M. (1968). Dimension and Production Relations of Trees and
757 Shrubs in the Brookhaven Forest, New York. *The Journal of Ecology*, *56*(1), 1–25.
758 <https://doi.org/10.2307/2258063>

759 Wolf, A., Anderegg, W. R., & Pacala, S. W. (2016). Optimal stomatal behavior with competition
760 for water and risk of hydraulic impairment. *Proceedings of the National Academy of*
761 *Sciences USA*.

762 Xu, X., Medvigy, D., Powers, J. S., Becknell, J. M., & Guan, K. (2016). Diversity in plant
763 hydraulic traits explains seasonal and inter-annual variations of vegetation dynamics in
764 seasonally dry tropical forests. *New Phytol.* <https://doi.org/10.1111/nph.14009>

765 Yang, J., Medlyn, B. E., De Kauwe, M. G., & Duursma, R. A. (2018). Applying the concept of
766 ecohydrological equilibrium to predict steady-state leaf area index. *Journal of Advances in*
767 *Modeling Earth Systems*. <https://doi.org/10.1029/2017MS001169>

768 Yarie, B. J., Kane, E., & Hall, B. (2007). Aboveground Biomass Equations for the Trees of
769 Interior Alaska, (January).

770 Zaehle, S., Sitch, S., Prentice, I. C., Liski, J., Cramer, W., Erhard, M., ... Smith, B. (2006). The
771 importance of age-related decline in forest NPP for modeling regional carbon balances.

772 *Ecological Applications*, 16(4), 1555–1574. <https://doi.org/10.1890/1051->
773 0761(2006)016[1555:TIOADI]2.0.CO;2
774 Zanne, A. E., Lopez-Gonzalez, G., Coomes, D. A., Ilic, J., Jansen, S., Lewis, S. L., ... Chave, J.
775 (2009). Global wood density database. *Dryad*. Identifier:
776 [Http://Hdl.Handle.Net/10255/Dryad.235](http://hdl.handle.net/10255/Dryad.235).
777 Zianis, D., Muukkonen, P., Mäkipää, R., & Mencuccini, M. (2005). *Biomass and Stem Volume*
778 *Equations for Tree Species in Europe*. The Finnish Society of Forest Science, The Finnish
779 Forest Research Institute. Retrieved from
780 <http://www.metla.fi/silvafennica/full/smf/smf004.pdf>

781

782

783 **Tables**

784 **Table 1:** Allocation and vegetation hydraulics characteristics in select vegetation models of
785 diverse scales

| Model | Type | Dynamic vegetation? | Plant hydraulics? | Leaf allocation | Reference |
|--------------------|------------|---------------------|-------------------|------------------|---|
| ACONITE | Big leaf | N | N | Flexible | (Thomas & Williams, 2014) |
| aDGVM | Individual | Y | N | Flexible | (Scheiter & Higgins, 2009) |
| CABLE | Big leaf | N | N | Fixed | (Wang et al., 2011) |
| CLM4 | Big leaf | N | N | Fixed (modified) | (Oleson et al., 2010) |
| CLM5 | Big leaf | N | Y | Fixed (modified) | (Lawrence et al., 2018) |
| CLM-FATES | Cohort | Y | N | Flexible | (Lawrence et al., 2018) |
| ED2 | Cohort | Y | N | Fixed | (Medvigy et al., 2009) |
| ED2-hydro | Cohort | Y | Y | Fixed | (Xu, Medvigy, Powers, Becknell, & Guan, 2016) |
| Hybrid 3.0 | Individual | Y | N | Flexible | (Friend, Stevens, Knox, & Cannell, 1997) |
| JeDi-DVGM | Big leaf | Y | N | Fixed | (Pavlick, Drewry, Bohn, Reu, & Kleidon, 2013) |
| LM3-PPA | Cohort | Y | N | Fixed (modified) | (Weng et al., 2015) |
| LPJ-DVGM | Cohort | Y | N | Flexible | (Sitch et al., 2003) |
| LPJ-Magnani Hybrid | Cohort | Y | N | Flexible | (Magnani, Mencuccini, & Grace, 2000; Zaehle et al., 2006) |

| | | | | | |
|-----------|------------|---|---|----------|---|
| ORCHIDEE | Big leaf | Y | N | Flexible | (Friedlingstein, Joel, Field, & Fung, 1999; Krinner et al., 2005) |
| SEIB-DGVM | Individual | Y | N | Flexible | (Sato, Itoh, & Kohyama, 2007) |
| TREES | Individual | N | Y | Flexible | (Mackay et al., 2015) |

786

787

788 **Table 2:** Fixed allocation models

| Model | Detailed description of leaf allocation |
|-------|--|
| CABLE | Big leaf model with fixed allocation coefficients. Annual NPP productivity is determined from annual carbon assimilation corrected for respiratory losses. The growth/decay of biomass during the steady state part of the growing season is determined by partitioning of NPP between leaves, roots and wood according to PFT-specific fixed coefficients. |
| CLM4 | Big leaf model with a modified version of fixed allocation coefficients. After accounting for the carbon costs maintenance respiration, remaining photosynthetic carbon can be allocated to new growth. Allocation to new growth is calculated for all of the plant carbon and nitrogen state variables based on specified C:N ratios for each tissue type and allometric parameters that relate allocation between various tissue types. Leaf carbon allocation is a dynamic function of NPP where the ratio of new to stem to new leaf growth (a) is $a = \frac{2.7}{1 + \exp(-0.004NPP - 300)} - 0.4,$ where NPP an annual value summed over the previous year. This results in increased woody allocation in high NPP environments. |
| CLM5 | Big leaf model with a modified version of fixed allocation coefficients. After accounting for the carbon costs maintenance respiration, remaining photosynthetic carbon can be allocated to new growth. Allocation to new growth is calculated for all of the plant carbon and nitrogen state variables based on specified C:N ratios for each tissue type and allometric parameters that relate allocation between various tissue types. Leaf carbon allocation is a dynamic function of NPP where the ratio of new to stem to new leaf growth (a) is $a = \frac{2.7}{1 + \exp(-0.004NPP - 300)} - 0.4,$ where NPP is an annual value summed over the previous year. This results in increased woody allocation in high NPP environments. |

| | |
|-----------|---|
| ED2 | <p>Cohort-based model. After accounting for respiration costs, remaining photosynthetic carbon can be allocated to new growth. During the steady state part of the growing season, allocation is determined by a functional relationship dependent on cohort dbh and PFT-specific leaf-dbh biomass relationships</p> $bl = a \cdot dbh^b,$ <p>where bl is leaf biomass and a and b are fixed PFT-specific constants.</p> |
| ED2-hydro | <p>Cohort-based model. After accounting for respiration costs, remaining photosynthetic carbon can be allocated to new growth. During the steady state part of the growing season, allocation is determined by a functional relationship dependent on cohort dbh and PFT-specific leaf-dbh biomass relationships</p> $bl = a \cdot dbh^b,$ <p>where bl is leaf biomass and a and b are fixed PFT-specific constants.</p> |
| JeDi-DVGM | <p>Big leaf model where carbon allocation to each tissue pool is proportional to the size of the storage pool. Allocation is determined by fixed coefficients that are PFT-specific, range from 0 to 1, and are mathematically constrained such that they sum to less than 1. The allocation coefficient fraction is designed to represent functional trade-offs in allocation: A higher allocation to fine roots enhances plant water uptake ability, but this comes at the expense of allocation to the above-ground tissues, decreasing the ability to capture light for photosynthesis.</p> |
| LM3-PPA | <p>Cohort-based model where empirical allometric equations that are PFT-specific and dependent on cohort dbh relate woody biomass (including coarse roots, bole, and branches), crown area, and stem diameter. Another set of fixed equations relate leaf mass to crown area and root mass to leaf mass. The target crown LAI that is set by PFT-specific equations and cohort light status (e.g. understory versus overstory).</p> |

789

790

791

Table 3: Flexible allocation models

| Model | Detailed allocation description |
|---------|---|
| ACONITE | <p>Big leaf model. At each daily time step, instantaneous carbon (C) return is calculated (which accounts for gross photosynthesis, growth respiration, and maintenance respiration of additional leaf allocation) to determine whether investing further C and nitrogen (N) in foliage will result in a positive C net uptake (up to some maximum leaf carbon which is set</p> |

| | |
|------------|---|
| | <p>on an annual timescale). If the maximum leaf allocation has been reached or N limits further leaf allocation, C is allocated to fill storage, grow wood, or increase fine roots. Further surplus C is allocated for fixation. At the end of each annual cycle, integrated annual marginal carbon return is used to recompute maximum leaf C and N and maximum root C and N. The marginal changes to photosynthesis from added leaf C, added leaf N, and added leaf C and N together are iterated over using to determine the marginal carbon return.</p> |
| aDGVM | <p>Individual-based mode. After covering respiratory costs, carbon is allocated to root, stem, or leaf in response to limiting resources (i.e. light-limited trees preferentially allocate to stem, water limited trees preferentially allocate to roots, photosynthetically-limited trees preferentially allocate to leaves). Thus, allocation is responsive to environmental conditions according to the following relations:</p> $a_R = \frac{1 + a_{0R} - G_i}{3 + a_{0R} + a_{0S} - Q_i - G_i - C_i}, a_S = \frac{1 + a_{0S} - Q_i}{3 + a_{0R} + a_{0S} - Q_i - G_i - C_i}, a_L = \frac{1 - C_i}{3 + a_{0R} + a_{0S} - Q_i - G_i - C_i}$ <p>where a_R, a_S and a_L describe carbon allocated to roots, stems and leaves, respectively, a_{0R}, a_{0S}, and a_{0L}, describe the fractions of carbon allocated to roots, stems and leaves when resources are not limiting. Q_i ranges from 0 to 1 (where 1 is no light limitation) and describes the light status of the plant and is based on the relative height of a given plant and its competitor. G_i is the weighted mean soil moisture index of all soil layers that a plant's roots have access to. C_i describes the deviance of leaf biomass from the fraction of leaf biomass in the nonlimiting case.</p> |
| CLM-FATES | <p>Cohort-based model where photosynthetic carbon is allocated according to the following hierarchy: Priority is given to maintenance respiration, followed by tissue maintenance and storage, then allocation to live biomass and then to the expansion of structural and live biomass pools. The maximum carbon allocation to leaf biomass and other tissues is determined using allometric constants, a scheme based on the ED model. However, target leaf biomass includes an optimization based “trimming” factor that allows for removal of leaves in negative carbon balance within the canopy due to light limitation. If the annual maintenance cost of the lowest leaf layer is less than the carbon gain, the canopy is trimmed by an increment which is applied up through the next calendar year.</p> |
| Hybrid 3.0 | <p>Individual-based model. If annual net carbon balance is positive (after allowing for carbon required to cover respiration and turnover costs), this carbon is allocated to new growth and growth respiration. Allocation occurs assuming (i) a fixed allometric relationship between diameter at breast height and woody carbon mass, (ii) that leaf area is linearly proportional to sapwood area at breast height, and (iii) that there is a fixed ratio between leaf and fine root masses. Allocation coefficients are PFT specific. The carbon balance of the lowest leaf layer</p> |

| | |
|--------------------|---|
| | of each tree crown is calculated daily. If, at the end of each year, carbon balance is negative, the leaf area is reduced by the amount present in the bottom leaf layer This results in the foliage area being optimized on an annual timestep based on carbon gain. |
| LPJ-DVGM | Cohort-based model. After accounting for maintenance and growth respiration and annual reproductive costs, the remaining carbon is available for producing new tissue. Scaling rules constrain allocation among leaves, fine roots and sapwood. First, leaf area is related to sapwood area through a constant. Second, rooting biomass is related to leaf biomass through a fixed coefficient and a water limitation factor that is an annual average value ranging between 0 and 1 that is used in calculating this year's leaf to fine root mass ratio for the allocation routine. Thus, water-limited environments require plants to allocate relatively more resources to fine root biomass compared to leaves. This results in increased respiration costs associated with roots and a loss of photosynthetic potential as the cost of having to acquire water and nutrients. |
| LPJ-Magnani Hybrid | Cohort-based model where allocation of carbon to conductive sapwood and absorbing roots is optimal with respect to achieving minimal whole-plant leaf-specific hydraulic resistance whilst supporting a maximum of transpiring leaf-tissue. Increased allocation to fine roots with tree height decreases below-ground plant hydraulic resistance which compensates for the increase in leaf-specific resistance of the stem with tree height, maintaining a constant whole-plant leaf-specific hydraulic conductance. Increasing respiratory costs relative to carbon gain to maintain whole-plant leaf-specific hydraulic conductance with increasing tree height reduces growth efficiency, resulting in a decline in productivity. |
| ORCHIDEE | Big leaf model where carbon is allocated to root, stem, and leaf in response to limiting resources (i.e. water, light, nitrogen): water, light, and nitrogen availability. No carbon is allocated to leaves when the LAI is above a PFT-specific annual maximum. Allocation is specified as: $a_R = 3a_{0R} \frac{L}{L + 2\min(W,N)}, a_S = 3a_{0S} \frac{\min(W,N)}{2L + \min(W,N)}, a_L = 1 - a_S - a_R,$ where a_R , a_S and a_L describe carbon allocated to roots, stems and leaves, respectively, a_{0R} , and a_{0S} describe the fractions of carbon allocated to roots and stems when resources are not limiting. Both a_{0R} , and a_{0S} are set to 0.3, giving a leaf allocation of 0.4 under conditions where resources are totally non-limiting. Resource availabilities of Light (L), water (W), and nitrogen (N) range from 0.1 (severely limited) to 1.0 (readily available) where W is dependent on monthly soil water content, L is dependent on canopy LAI, and N is assumed to be a function of soil temperature and soil moisture. |
| SEIB-DGVM | Individual-based model where growth and allocation occur at three separate time scales. At the daily time scale, after respiratory costs are accounted for, leaf and fine root turnover is |

| | |
|-------|--|
| | replenished according to fixed ratios between leaf and fine root biomass. Leaf biomass is constrained by two functional relationships based on fixed, PFT-specific coefficients and carbon availability. Functional relationships include maximum crown surface area and maximum cross-sectional area of sapwood. Trunk growth and expansion of crown area occur at the monthly timescale according to fixed constants and PFT-specific allometric relationships. At the annual-level, the height of the lowest branch increases as a result of self-pruning of the bottom of the crown layer. During pruning, a maximum of 10 crown disks can be pruned at one time, each at a depth of 10cm. Crown disks are purged based on the expected profit (carbon gain) of a particular crown disk. |
| TREES | Individual-based model. After accounting for respiration costs, remaining photosynthetic carbon can be allocated to new growth. Leaf turnover is dependent on hydraulic impairment of the lateral stem: $L_M = \begin{cases} L_0 M, & P_L \geq 0.5 \wedge c_{ls} \leq c_{lrs} \\ P_L L_0 M, & P_L < 0.5 \wedge c_{ls} > c_{lrs} \end{cases}$ where L_0 is initial leaf area index, M is unstressed leaf mortality rate, P_L is lateral stem proportional loss of conductivity, and c_{ls} and c_{lrs} are, respectively, and the Weibull c parameters for the lateral stem and the lateral shallow root. Allocation to stem is fixed. |

792

793 **Figure Captions**

794

795 **Figure 1.** Taxonomic scales of variation in leaf area divided by tree basal area ($A_L:BA$)
796 compared to another widely-used plant functional trait, wood density (WD), recorded in the
797 Biomass and Allometry Database for woody plants (Falster et al., 2015) and the Global Wood
798 Density Database (Zanne et al., 2009). Horizontal dashed line represents the fraction of within-
799 species variation in $A_L:BA$ explained by plant height.

800

801 **Figure 2.** Leaf allocation and gas exchange jointly affect plant productivity. (a) Model scheme
802 of plant hydraulic transport, illustrated per standard electrical resistance diagrams with
803 conductivity ($K=1/\text{resistance}$) and water potential of soil, stem and leaf (Ψ) under normal
804 conditions. (b) Schematic of possible plant physiological adjustments at the leaf- and stem-level
805 made in response to increased leaf water demand under water-limited conditions. (c) Changes in
806 C_i and stomatal conductance with increasing allocation to leaf area relative to water transport

807 tissue ($A_L:A_S$). Note that these trends are for a tree modeled using a single resistor representing
808 whole-plant hydraulic transport up to the substomatal cavity and a hydraulic optimization-based
809 stomatal conductance model (Trugman, Detto, et al., 2018). Given multiple resistances specific
810 to roots, stem, and leaves, trends are broadly similar but exhibit a delay the predicted declines in
811 stomatal conductance (g_s) and intercellular CO_2 (C_i) with increased $A_L:A_S$ (Hubbard et al., 2001;
812 Sperry, 2000). (d) Whole-tree gross primary productivity (GPP) and carbon costs associated with
813 respiration and turnover with increased $A_L:A_S$. (e) Total whole plant carbon gain (photosynthesis
814 minus respiration and turnover costs). Maxima indicates the maximum tree carbon gain given
815 fixed environmental conditions.

816

817 **Figure 3.** Tree fitness quantified through whole tree carbon gain (photosynthesis minus
818 respiration and turnover costs) for trees of the same size under wet (solid green lines) and dry
819 (solid tan lines) conditions. Maxima indicate the maximum tree carbon gain given fixed
820 environmental conditions and photosynthesis and hydraulic traits. Individual variation in carbon
821 gain can occur through adjustment of allocation to leaf area relative to water transport tissue
822 ($A_L:A_S$) to adapt to changes in water availability. Local optima for $A_L:A_S$ for trees with identical
823 traits but either in wetter or drier conditions are indicated with dashed vertical lines of the same
824 color. These fitness curves were generated using the HOTTER model (Trugman, Detto, et al.,
825 2018).

826

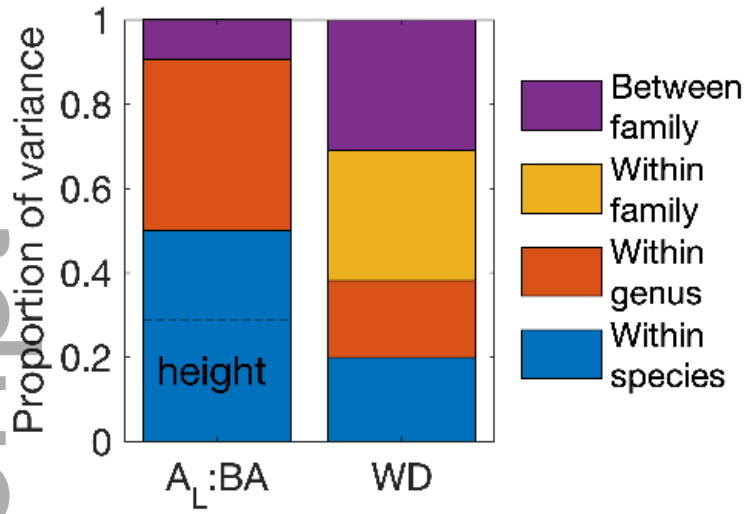
827 **Figure 4.** Empirical representations of leaf allocation can result in substantial uncertainty in
828 predictions for plant biomass accumulation depending on the local climatic conditions.
829 Ecosystem Demography model version 2 (ED2)-predicted aspen basal area accumulation over a
830 200-year spin up for trees with two different site-specific leaf allometries, one derived from trees
831 sampled in central Alaska (Yarie et al., 2007) and one derived from trees sampled in central
832 Canada (Bond-Lamberty et al., 2002), that constrain tree leaf carbon allocation strategy. This
833 figure illustrates how model predictions can vary dramatically based on the allometric constraints
834 used for simulations, highlighting the need for a more holistic understanding of leaf allocation.

835

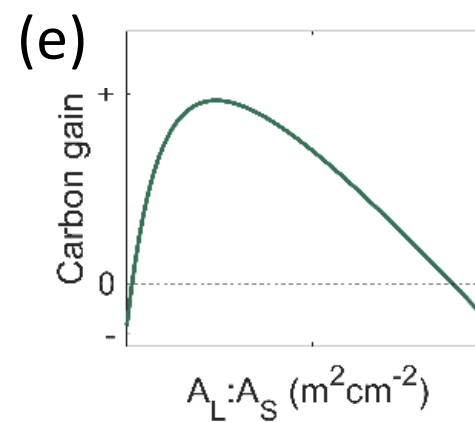
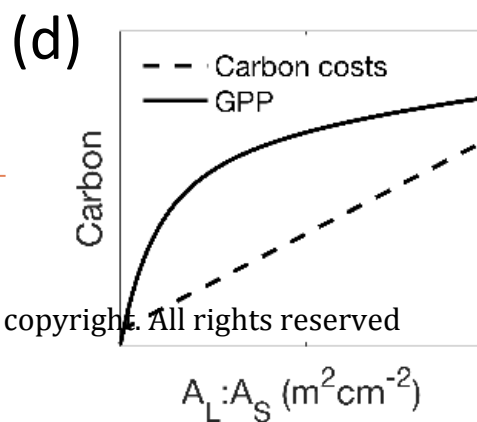
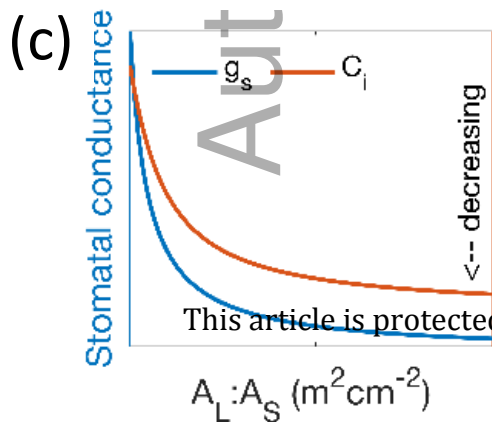
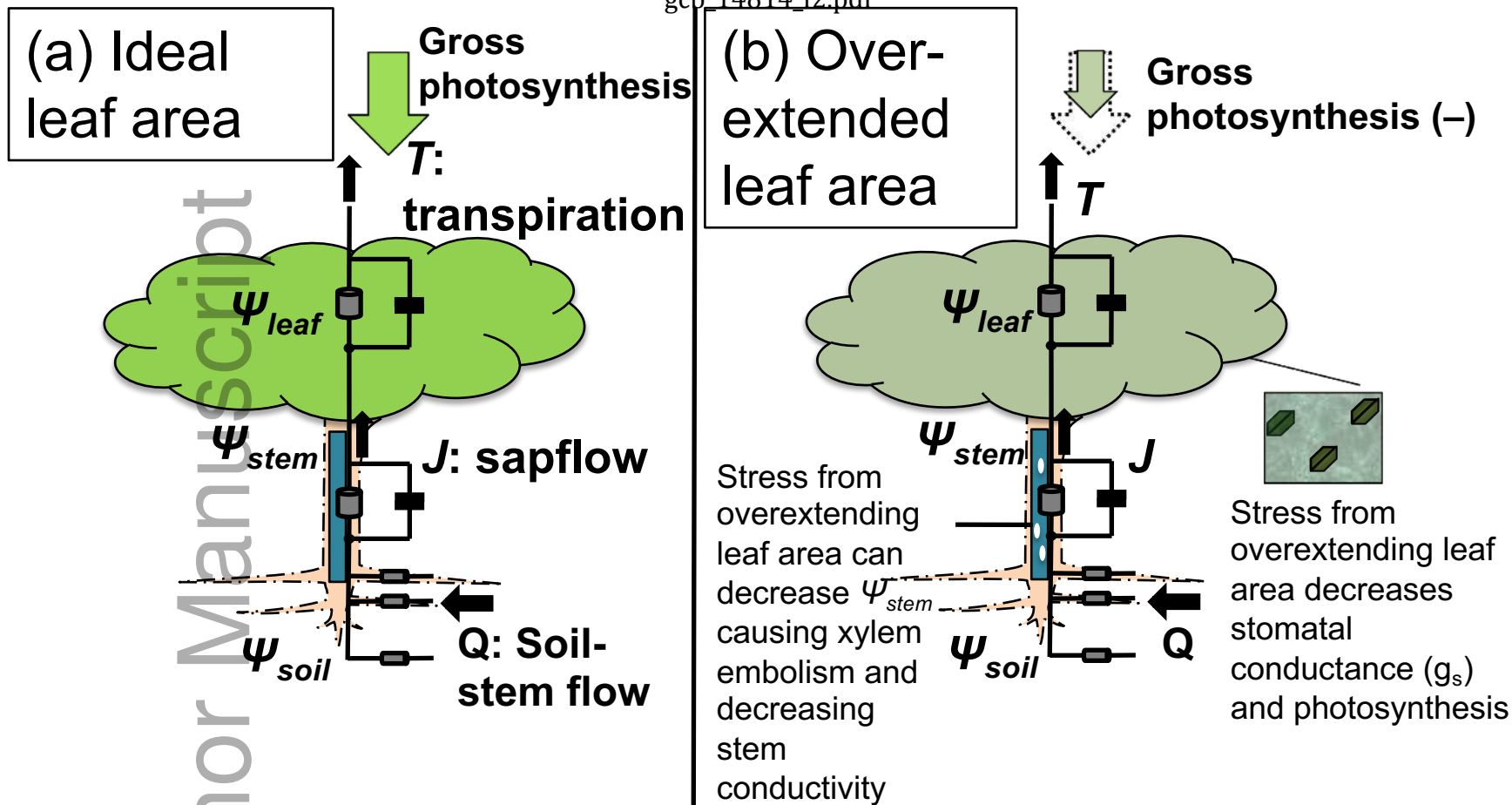
836 **Figure 5.** Schematic of expected allocational responses to various resource limitations and
837 impacts of allocation strategy on marginal plant fitness increase. (a) Expected changes in root,

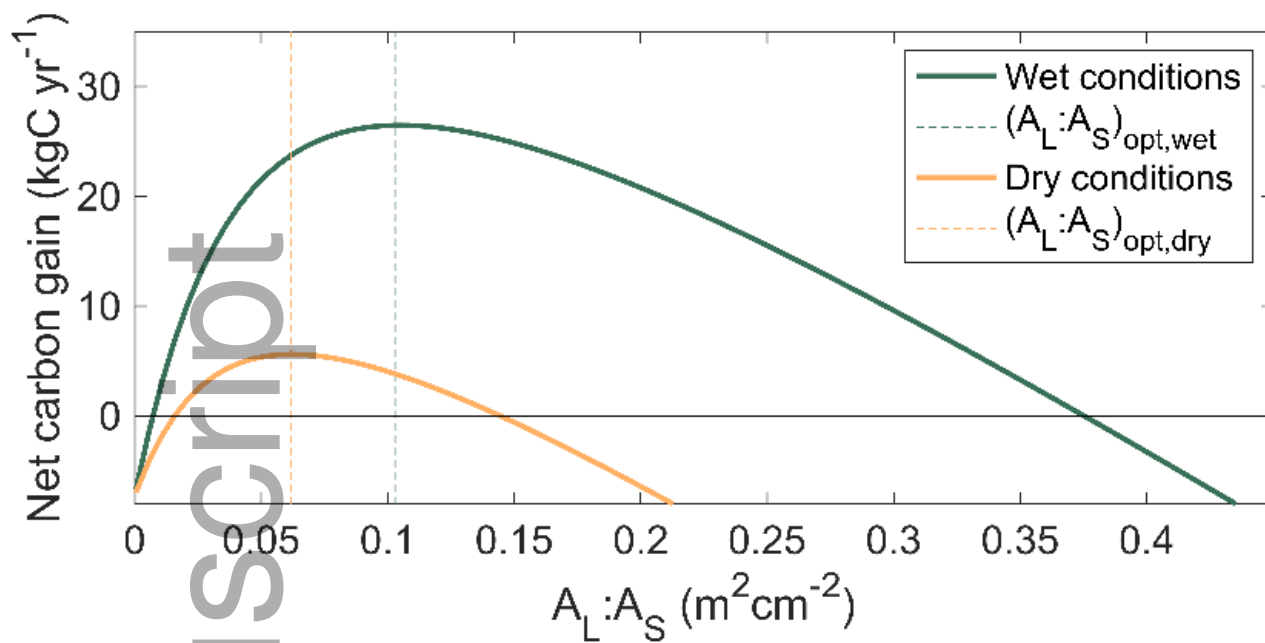
838 leaf, and stem allocation in response to increased competition for light, decreased soil water
839 availability, and decreased nutrient availability. Pluses combined with solid lines indicate
840 increased carbon allocation to a given tissue and minuses combined with dashed lines indicate
841 decreased allocation. **(b)** Schematic of fitness as a function of relative carbon allocation (in
842 percent) to leaf, root, and stem tissue including a hypothetical optimum for a given set of local
843 environmental conditions. Solid arrows indicate directional shifts in relative allocation in
844 response to increased water availability, decreased nutrient availability, and decreased light
845 availability.

Author Manuscript

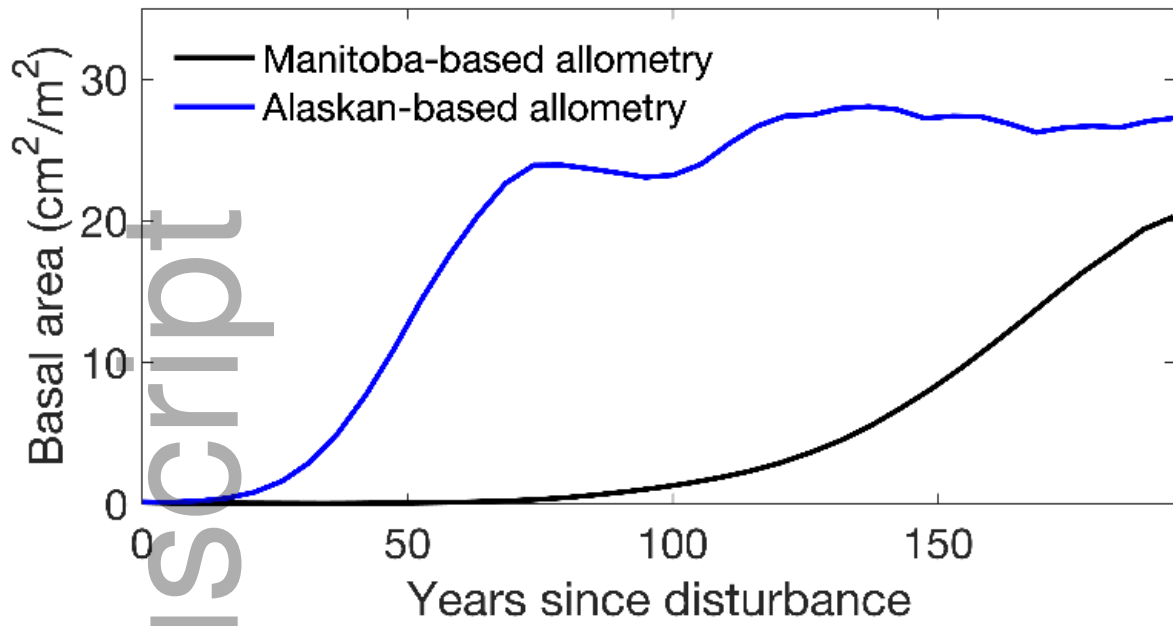


gcb_14814_f1.tiff





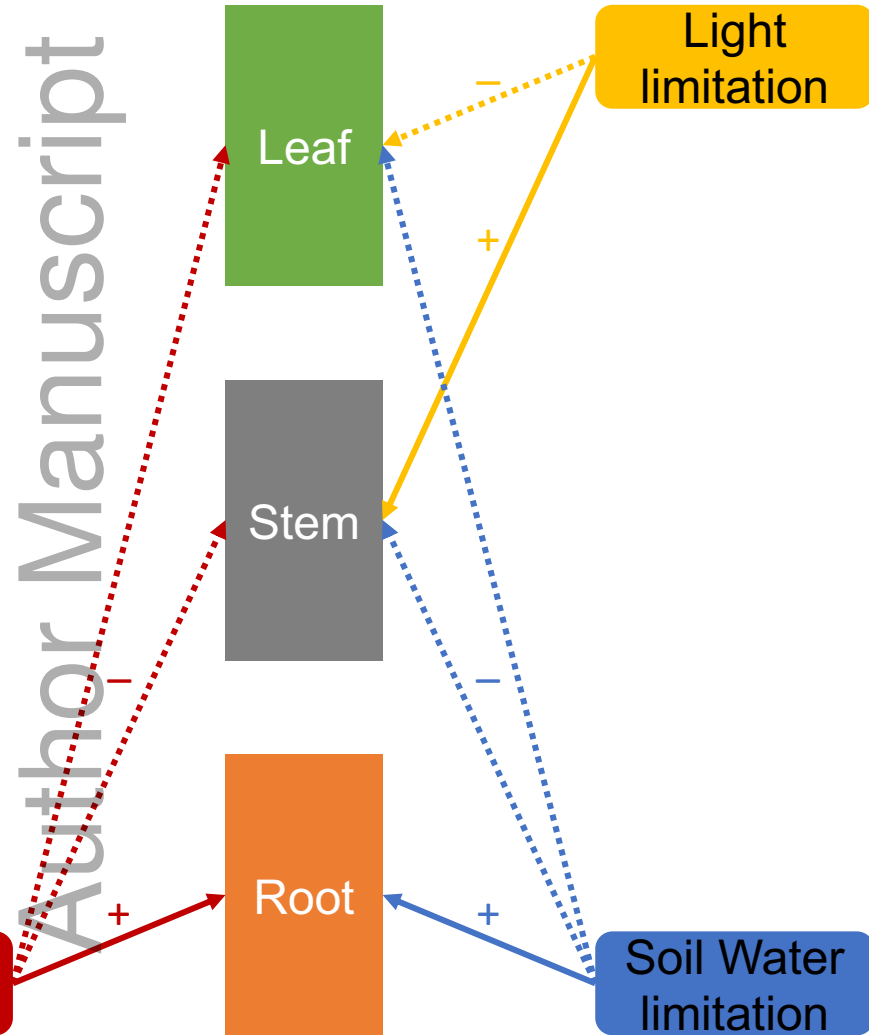
gcb_14814_f3.tiff



gcb_14814_f4.tiff

Author Manuscript

(a)



(b)

